Orexin/hypocretin system modulates amygdala-dependent threat learning through the locus coeruleus

Robert M. Sears[a,1], Ann E. Fink[a,2], Mattis B. Wigestrand[a,b,2], Claudia R. Farb[a], Luis de Lecea[c], and Joseph E. LeDoux[a,d,1]

[a]Center for Neuroscience, New York University, New York, NY 10003; [b]Department of Molecular Biosciences, University of Oslo, 0371 Oslo, Norway; [c]Neurosciences Program and Departments of Psychiatry and Behavioral Sciences, Stanford University, Stanford, CA 94305; and [d]Emotional Brain Institute, Nathan Kline Institute for Psychiatric Research, Orangeburg, NY 10962

Contributed by Joseph E. LeDoux, October 31, 2013 (sent for review September 5, 2013)

Survival in a dangerous environment requires learning about stimuli that predict harm. Although recent work has focused on the amygdala as the locus of aversive memory formation, the hypothalamus has long been implicated in emotional regulation, and the hypothalamic neuropeptide orexin (hypocretin) is involved in anxiety states and arousal. Nevertheless, little is known about the role of orexin in aversive memory formation. Using a combination of behavioral pharmacology, slice physiology, and optogenetic techniques, we show that orexin acts upstream of the amygdala via the noradrenergic locus coeruleus to enable threat (fear) learning, specifically during the aversive event. Our results are consistent with clinical studies linking orexin levels to aversive learning and anxiety in humans and dysregulation of the orexin system may contribute to the etiology of fear and anxiety disorders.

norepinephrine | fear conditioning | channelrhodopsin-2

Hess and Akert demonstrated that electrical stimulation of the perifornical (PFH) region of the hypothalamus elicits defensive or aggressive responses in cats (1). Others showed that hypothalamic stimulation can serve as the aversive unconditioned stimulus (US) (2), indicating that the hypothalamus processes threat information important for aversive learning. One possibility is that orexin neurons, which populate these hypothalamic areas, may mediate these observed responses, as these neurons project to and modulate brain areas critical for threat processing, reward, and memory.

Orexins are neuropeptides produced in the PFH and lateral regions of the hypothalamus (LH) (3, 4). Two orexin peptides (Orexin-A and Orexin-B) are processed from one peptide precursor (prepro-orexin) and bind two distinct G protein–coupled receptors (OrxR1 and OrxR2) in the brain (3, 4). Activation of either receptor commonly increases excitability in target neurons by reducing potassium channel conductance, enhancing presynaptic glutamate release, or increasing postsynaptic NMDA receptor (NMDAR) conductance (5, 6). Orexin receptors are differentially distributed in the brain and may serve differing roles in stress, arousal, vigilance, feeding, reward processing, and drug addiction (7–10). Evidence suggests that, in general, OrxR2 is involved in maintenance of arousal or wakefulness (11, 12), whereas OrxR1 mediates responses to environmental stimuli (13, 14).

Recent reports point to a role for the orexin system in emotional regulation. Overactivity in orexin neurons can exacerbate panic-like episodes and lead to an anxiety-like phenotype in rats (15, 16). Conversely, administration of the dual orexin receptor antagonist almorexant blunts autonomic and behavioral responses affiliated with heightened stress levels (17, 18). Although orexin system activity is linked to general states of hyperarousal, the precise role of orexin in these and other aversive states remains unknown.

Hypothalamic orexin neurons send a dense output to the locus coeruleus (LC) and depolarize neurons in vitro and in vivo (19–21). In line with their connectivity, LC neurons respond to phasic stimuli in a manner comparable to orexin neurons (22), suggesting that orexin neurons modulate LC responses to salient sensory events. Interestingly, orexin and LC neurons are both activated by aversive stimuli such as shock (23, 24). Thus, orexin could contribute to aversive learning by way of LC, given the importance of norepinephrine to aversive memory processes in amygdala (25–27).

Pavlovian threat (fear) conditioning is a well-established behavioral paradigm to assess the formation, storage, and expression of aversive memories (28). During training, animals learn to associate an aversive US, such as a footshock, with a neutral conditioned stimulus (CS), such as a tone, when both occur in close temporal proximity. Here, we tested the hypothesis that orexin neurons phasically activate locus coeruleus neurons during an aversive event to enable threat learning. Using a combination of behavioral pharmacology, electrophysiology, and optogenetic approaches, we show that orexin neurons, via activation of OrxR1 in the LC, facilitate the acquisition of amygdala-dependent threat memory.

Results

Regulation of Threat Learning by the Orexin System. To test the hypothesis that orexin carries information important for aversive memory formation, we blocked OrxR1 activity at various phases of an auditory threat conditioning paradigm. We administered the OrxR1 antagonist SB 334867 by intracerebroventricular (ICV) infusion before threat conditioning and examined conditioned freezing behavior, a general reaction to perceived threat (29), in a long-term memory (LTM) test (Fig. 1*A*). When SB 334867 infusions were made before training, freezing was

Significance

The hypothalamic orexin (hypocretin) system controls survival-related processes such as food intake, arousal, and stress. Here we show that orexins also play an important role in learning about stimuli that predict harm. We demonstrate that blocking orexin activity in the noradrenergic locus coeruelus (LC) reduces, whereas increasing its activity enhances, threat learning in a Pavlovian auditory threat conditioning paradigm. Moreover, we demonstrate a direct functional connection between orexin enhancement of LC activity and amygdala-dependent memory processes. Strong, aversive memories can lead to fear and anxiety disorders that have a negative impact on individuals and their quality of life. The orexin system may represent a unique treatment target for these disorders.

Author contributions: R.M.S., A.E.F., M.B.W., and J.E.L. designed research; R.M.S., A.E.F., M.B.W., and C.R.F. performed research; L.d.L. contributed new reagents/analytic tools; R.M.S., A.E.F., M.B.W., and J.E.L. analyzed data; and R.M.S., A.E.F., and M.B.W. wrote the paper.

The authors declare no conflict of interest.

Freely available online through the PNAS open access option.

[1]To whom correspondence may be addressed. E-mail: robert.sears@nyu.edu or ledoux@cns.nyu.edu.

[2]A.E.F. and M.B.W. contributed equally to this work.

This article contains supporting information online at www.pnas.org/lookup/suppl/doi:10.1073/pnas.1320325110/-/DCSupplemental.

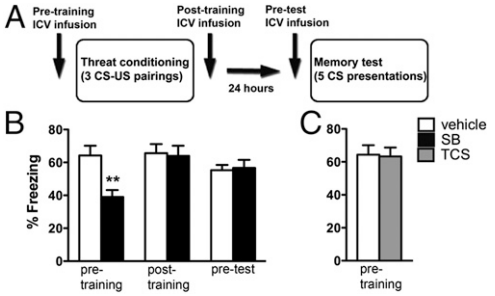

Fig. 1. Orexin signaling through OrxR1 is required for normal threat learning. (*A*) Schematic indicating the timeline for drug treatments, training, and LTM test. Vertical arrows indicate time of infusion for each manipulation. (*B*) Mean freezing data during LTM (total percent time freezing during five 30-s bins) for pre- (n = 7–15/group) and posttraining (n = 5–7/group), as well a pretest infusions (n = 8/group) of the OrxR1 antagonist SB 334867 (labeled SB; 5 μg). Only pretraining infusions yielded a significant change in LTM. Pre-CS baseline values were not statistically different between groups and therefore were not included in the graph. (*C*) Infusion of the OrxR2 antagonist TCS-OX2-29 (labeled TCS; 5 μg) before conditioning had no effect on LTM. All bars indicate mean ± SEM. $^{**}P < 0.01$, unpaired Student t test.

impaired during LTM [Fig. 1*B*, *Left*, n = 7–16/group, 5 μg/side, 64.3 ± 6% vs. 39.1 ± 4% freezing, Student t Test, $t(20) = 3.429$, $P = 0.003$], demonstrating that OrxR1 activation is required for normal formation of threat memories. To rule out potential drug effects during the consolidation phase, because the drug was administered before training, we infused SB 334867 immediately following training and found no effect on LTM freezing behavior [Fig. 1*B*, *Center*, n = 5–7/group, 5 μg/side, 66 ± 6% vs. 64 ± 6% freezing, Student t test, $t(10) = 0.199$, $P = 0.85$]. Similarly, SB 334867 infusion before the LTM test did not significantly influence expression of conditioned freezing [Fig. 1*B*, *Right*, n = 8/group, 5 μg/side, 55 ± 3% vs. 56.7 ± 5% freezing, Student t test, $t(14) = 0.238$, $P = 0.82$]. These data show that OrxR1 activation, specifically during the training phase, is required for normal threat memory formation.

We hypothesized that OrxR1 activation is responsible for the effect of SB 334867 on acquisition of threat memory but could not rule out a nonselective effect of the drug on OrxR2 receptors. To test whether OrxR2 contributes to aversive learning, animals were infused with the selective OrxR2 antagonist TCS-OX2-29 at an effective dose before training (30). We found no effect on learning, suggesting that OrxR2 signaling is not involved in the acquisition or consolidation of threat-conditioned memories [Fig. 1*C*; n = 8/group, 5 μg/side, 64 ± 6% vs. 63 ± 5%, Student t test, $t(14) = 0.131$, $P = 0.89$]. Taken together, these data suggest that central signaling by orexin via OrxR1 is critical for the learning but not for the consolidation or expression of aversive memories.

Orexin Signaling in the LC Mediates Threat Learning. Behavioral pharmacology experiments revealed no direct role for OrxR1 signaling in lateral nucleus of the amygdala (LA) in the acquisition of threat memories [n = 8/group, 1 μg/side, 69.5 ± 5% vs. 69.2 ± 5%, Student t test, $t(14) = 0.038$, $P = 0.970$], consistent with findings showing sparse orexin projections to the LA and minimal receptor expression (10, 31). Because orexin projections and OrxR1s are dense in the LC, orexin positively modulates LC neurons (19, 20), and the LC, is a major source of the catecholamine norepinephrine, which is strongly implicated in aversive memory formation (25, 26, 32), we hypothesized that local blockade of OrxR1 in LC exclusively during the training phase would impair threat memory formation. Consistent with this prediction, pharmacological blockade of OrxR1 signaling in LC before conditioning [Fig. 2*B*; n = 5–10/group, 300 ng or 1 μg/side; vehicle: 73.1 ± 4% vs. 300 ng: 73.2 ± 4% vs. 1 μg: 47.9 ± 3% freezing, one-way ANOVA, $F(2,23) = 19.79$, Tukey's multiple comparison test, $P < 0.001$], but not immediately after conditioning [Fig. 2*C*; n = 5/group, 1 μg/side, 72 ± 6% vs. 79 ± 5%, $t(7) = 0.883$, $P = 0.41$], reduced threat memory formation, suggesting that OrxR1 signaling in LC is required during the training phase. Importantly, these results were not due to shock sensitivity (Fig. S1), and off-site infusions of SB 334867 did not produce this behavioral effect [Fig. S2*A*; n = 14/group, 63 ± 5% vs. 64 ± 5% freezing, Student t test, $t(26) = 0.129$, $P = 0.89$], thus confirming the behavioral specificity, site specificity, and, to an extent, the dose used in the observed results. To further corroborate these findings, we next assessed short-term-memory (STM) before consolidation (33). If OrxR1 signaling is required for acquisition, pretraining blockade of OrxR1 should influence STM in addition to LTM. Indeed, we found that SB 334867 infusion before training reduced STM freezing [Fig. 2*D*; n = 14–20/group, 1 μg/side, 81 ± 3% vs. 61 ± 3% freezing, Student t test, $t(32) = 4.786$, $P < 0.001$], further supporting the hypothesis that OrxR1 signaling is important during the learning phase of aversive memory formation.

Optogenetic Activation of Orexin Fibers Causes Rapid, Direct Excitation of Cells in the LC. Studies have described a direct functional connection between orexin neurons and the LC, although the behavioral consequences of orexin neuron manipulations have not been explored until recently. We selectively expressed channelrhodopsin-2 (ChR2) (34) in orexin neurons and measured the effects of locally activating orexin terminals in the LC. We targeted the medial and PFH orexin fields due to evidence that these populations may be involved in aversive processing (13, 35), observing an infection efficiency of 45.06 ± 3.82% (n = 12 animals). After confirming viral expression in PFH orexin neurons (Fig. 3*B* and Fig. S3*A*), we ensured that we could obtain consistent photo-activation of ChR2-expressing orexin neurons by recording light-evoked action potentials from these cells in acute coronal brain slices. ChR2-expressing cells were clearly visible under wide-field fluorescence in acute slices (Fig. S3*A*). Optical activation of orexin cells elicited consistent and robust spiking in ChR2-expressing neurons (three of three cells; Fig. S3*B*), whereas no response was observed in any of the mCherry-expressing cells (n = 4), even at maximal light power.

As expected, we also observed fibers extending from infected orexin neurons to the LC (Fig. 3*C*). We used photo-activation of these ChR2-expressing axon terminals to elicit and characterize synaptic transmission from these fibers onto projection cells of

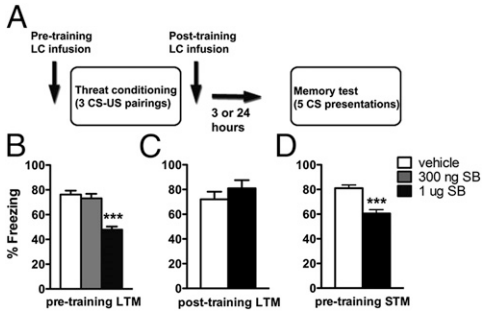

Fig. 2. OrxR1 blockade in the LC attenuates threat memory formation. (*A*) Schematic indicating the timeline for intra-LC drug treatments, training, and LTM test. (*B*) Pretraining infusions of 1 μg, but not 300 ng, of SB-334867 blunts LTM formation (n = 5–14/group). (*C*) Posttraining infusions of 1 μg SB 334867 had no effect on memory consolidation as measured by LTM. (*D*) Pretraining infusion of 1 μg SB 334867 significantly reduced STM, supporting a role for OrxR1 in memory acquisition. Bars indicate mean ± SEM. $^{**}P < 0.01$ relative to vehicle, $^{\#}P < 0.01$ relative to 300 ng SB 334867, one-way ANOVA followed by Tukey's multiple comparison test.

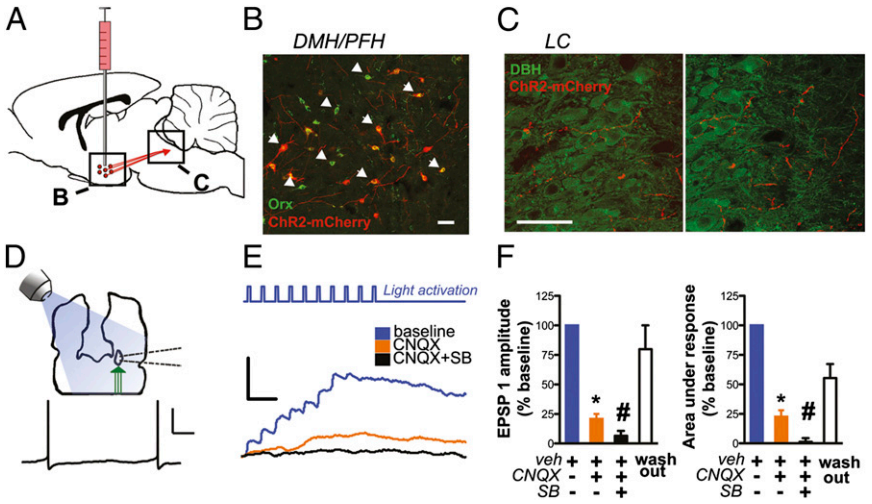

Fig. 3. In vitro stimulation of ChR2-expressing fibers from orexin-immunopositive neurons activates LC neurons. (*A*) Schematic depicting strategy for targeting orexin neurons in medial PFH and projections to LC. (*B*) Neurons in the hypothalamus transduced with LV-Hcrt::ChR2-mCherry colabel with mCherry (red) and orexin (green). Image depicts infected (arrow) and uninfected (arrowhead only) orexin-A immunopositive neurons. All infected cells were orexin-A immunoreactive. (Scale bar, 50 μM.) (*C*) mCherry-immunopositive fibers project to and innervate DBH-immunopositive neurons in LC. (Scale bar, 50 μM.) (*D*) (*Upper*) Schematic of recording from LC cells in a horizontal brainstem slice. (*Lower*) Spontaneous firing characteristic of LC neurons used to identify cells after patching. Calibration bars: 200 ms and 40 mV. (*E*) Averaged traces (five sweeps each) from a representative LC cell receiving orexin inputs; stimulation is a 10-pulse train of illumination at 20 Hz (pulse width = 10 ms). The blue line indicates the mean baseline response (in 0.1% DMSO), the orange line the response from the same cell after 15 min in CNQX (10 μM), and the black line the response after 10 additional min bathed in CNQX and SB 334867 (10 μM). Calibration bars: 100 ms and 5 mV. (*F*) (*Left*) Bar plot indicating the mean decrease in initial EPSP amplitude after application of CNQX and CNQX + SB 334867. (*Right*) Bar plot indicating a decrease in area under the synaptic response after application of CNQX and CNQX + SB 334867. The right bars in each plot represent values after 28 min of washout in control ACSF (0.1% DMSO). All values are normalized as a percent of the baseline response and are presented as mean ± SEM. One-way ANOVA, $^{*}P < 0.01$ CNQX vs. baseline, $^{\#}P < 0.05$ CNQX vs. SB + CNQX.

the LC. We obtained whole-cell current-clamp recordings from LC cell somata while optically stimulating the ChR2-infected axon terminals using a truncated protocol similar to that used in vivo (20-Hz train, 10-ms pulse duration, 10 pulses total) (36). Using optical stimulation alone, we were able to observe robust fast synaptic responses in a number of LC cells accompanied by a more long-lasting depolarization (Fig. 3*E*).

The fast component of the light-evoked synaptic response was measured by the maximal amplitude of the first excitatory postsynaptic potential (EPSP; *SI Materials and Methods*), and the slow component was measured by the area under the synaptic depolarization (Fig. 3*F*). Application of blockers of AMPA receptors and orexin receptors significantly decreased both the fast (one-way ANOVA, $F = 9.13$, $P < 0.001$) and slow (one-way ANOVA, $F = 8.84$, $P < 0.001$) components of depolarization ($n = 4$ cells from four animals). As expected based on previous work (37), a large component (79 ± 4%) of the fast EPSP was blocked after 15 min of incubation in 6-cyano-7-nitroquinoxaline-2,3-dione (CNQX) (10 μM) and therefore mediated by AMPA-type glutamate receptors (two-tailed paired comparison, $P = 0.004$). The area under the light-induced depolarization was also significantly reduced by CNQX (77 ± 5%), indicating significant summation of AMPA receptor-mediated EPSPs (two-tailed paired comparison, $P = 0.004$). Surprisingly, in these same cells, when the OrxR1 antagonist SB 334867 (10 μM) was bath-applied in conjunction with CNQX for 10 min, the remaining component (93 ± 4%) of the fast synaptic depolarization was largely abolished (two-tailed paired comparison with CNQX, $P = 0.045$). The addition of SB 334867 with CNQX completely abolished the long-lasting depolarization (99 ± 3%, two-tailed paired comparison with CNQX, $P = 0.02$), consistent with a prolonged, volume transmission-type effect of optically induced orexin release. These results demonstrate that orexin expressing cells of the PFH corelease both orexin and glutamate to mediate direct, rapid, and robust depolarization of LC cells.

In a separate set of experiments, we examined the effect of SB 334867 alone on similar light-evoked responses (Fig. S4). We observed that OrxR1 blockade in the absence of CNQX did not significantly change EPSP amplitude, although we observed a negative trend (Fig. S4*A*; EPSP amplitude = 75 ± 16% of baseline, $P = 0.11$, two-tailed paired comparison). We did not observe any trend when measuring the effect of SB alone on the area under the cumulative synaptic response (Fig. S4*B*; area = 103 ± 16% of baseline, $P = 0.85$, two-tailed paired comparison). The lack of effect due to SB alone could be explained by the variability inherent in the glutamatergic responses riding on the oscillating membrane potentials of LC neurons. To explore this possibility, we calculated the signal-to-noise ratio (SNR) of the predicted orexin contribution to the synaptic responses. As anticipated, the SNR of the orexin-mediated depolarization was near 1:1 in the presence of intact glutamatergic transmission (Fig. S4*C*). In the presence of CNQX, however, SNR increased to 1.94 ± 0.5 for the EPSP amplitude and 3.88 ± 1.2 for the area under the response. Thus, although the synaptic signature of orexin alone is small relative to the AMPA receptor–mediated response, the modest depolarizing bias provided by orexin could increase LC cell firing in response to synaptic inputs. The robust depolarization of LC cells provided by combined activation of glutamate and orexin receptors could significantly enhance learning in a threat conditioning paradigm.

Optogenetic Activation of Orexin Fibers in LC During Training Enhances Threat Learning. We next assessed the effect of optically activating ChR2-expressing orexin fibers in vivo. First, we photoactivated orexin fibers in LC and used c-Fos immunohistochemistry as a marker for neuronal activity (Fig. 4 *A* and *B*). We targeted the medial and PFH orexin fields due to evidence that these populations may be involved in aversive processing (13, 35), observing an infection efficiency of 45 ± 4% ($n = 12$ animals). Increased c-Fos expression was detected in dopamine beta hydroxylase (DBH)-immunopositive neurons of ChR2-mCherry–expressing

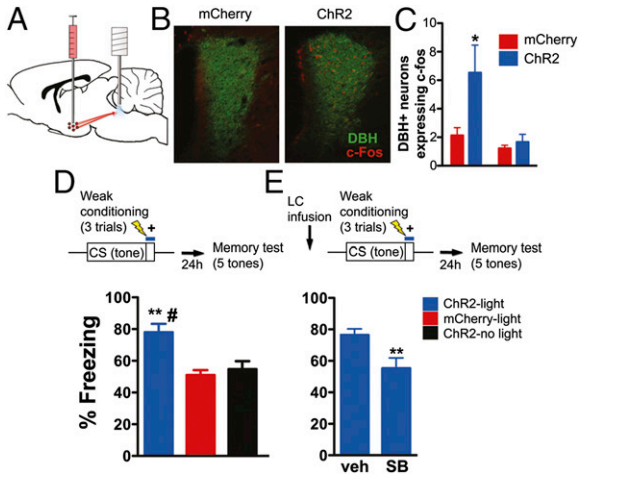

Fig. 4. Optical stimulation of orexin fibers in LC is sufficient to enhance threat memory formation. (*A*) Schematic of virus injection and illumination. Lentivirus expressing either ChR2-mCherry or mCherry alone in orexin neurons were injected in the medial PFH orexin field, with cannulae implanted above LC for fiber optic stimulation. (*B*) Optically evoked c-Fos expression in DBH-immunopositive (noradrenergic) neurons in LC. (*C* and *D*) Blue light stimulation of orexin fibers in LC enhances threat memory formation in ChR2-mCherry expressing animals but not mCherry controls. (*C*) c-Fos is increased only on the side of stimulation in ChR2-expressing animals compared with mCherry-expressing animals (averaged DBH and c-Fos colabeled neurons/slice, two-way ANOVA followed by Bonferonni posttest, $*P < 0.05$). (*D*) (*Upper*) Schematic of the weak threat conditioning protocol. (*Lower*) ChR2 stimulation of orexin-expressing axons enhances conditioning evoked by the weak protocol. (*E*) (*Upper*) Schematic of pretraining LC infusion relative to weak conditioning protocol. (*Lower*) Pretraining infusions of SB 334867 (1 μg) block blue light enhancement of threat learning in ChR2-expressing animals. Bar plots indicate mean ± SEM. Two-way ANOVA followed by Tukey's multiple comparison test, $**P < 0.01$ relative to mCherry-light and $^{\#}P < 0.01$ compared with ChR2-no light.

animals relative to mCherry-alone controls [Fig. 4*C*; $n = 6$/group, two-way ANOVA, interaction: $F(1,20) = 3.82$, $P = 0.06$, main effect of virus: $F(1,20) = 5.22$, $P = 0.03$; main effect of side: $F(1,20) = 12.75$, $P = 0.002$; Bonferonni posttest, $P < 0.05$ for ipsilateral side between ChR2-mCherry and mCherry animals]. These results, in combination with the slice electrophysiology data, demonstrate that optical stimulation of orexinergic axons evoke robust LC activation, allowing us to temporally regulate transmitter release from orexin terminals during threat conditioning trials.

To determine whether orexin fiber stimulation facilitates memory, we used a weak threat conditioning paradigm that produces lower levels of freezing than normal conditioning procedures (36). In the experimental group, brief optical stimulation of orexin expressing axons in LC co-occurred with tone-shock presentation at the end of each trial (20-Hz train, 10-ms pulse duration for 2 s; Fig. 4 *D* and *E*). Optically stimulated ChR2-expressing animals froze significantly more than both the animals expressing mCherry alone and no-light controls during LTM (78 ± 5% vs. 51 ± 3% vs. 55 ± 5%, respectively), suggesting that orexin fiber stimulation served to enhance threat memory formation [Fig. 4*D*; $n = 5$–7/group, one-way ANOVA, $F(2,17) = 8.79$, $P = 0.003$]. We observed no significant difference between the two control groups (ChR2 without light and mCherry with light) but a significant difference between controls and the experimental group (Tukey's multiple comparison test, mCherry-light vs. ChR2-light and ChR2-no light vs. ChR2; both $P < 0.01$). Therefore, only the combination of ChR2 and photoactivation lead to enhanced freezing during LTM. To confirm that orexin signaling through OrxR1 is responsible for our observations, ChR2-expressing animals were infused with either SB 334867 or vehicle in LC before training with blue light stimulation (Fig. 4*E*). OrxR1 antagonism significantly decreased the effects of optical stimulation [$n = 7$/group, 1 μg ipsilateral infusion, 76 ± 4% vs., 55 ± 7% freezing, Student t test, $t(12) = 2.771$, $P = 0.02$], suggesting that our behavioral results are due in large part to evoked orexin release in the LC.

Functional Disconnection of a Hypothalamic-LC-LA Circuit Impairs Threat Learning. To test whether the orexin-to-LC circuit influences aversive learning via downstream effects on the amygdala, we used a strategy whereby the hypothalamus-LC-LA circuit is pharmacologically disconnected at different nodes of the circuit during behavioral training (Fig. 5 *A* and *B*). In these experiments, activity in LC was unilaterally antagonized with SB 334867, whereas norepinephrine signaling was blocked unilaterally in LA with the β-adrenergic receptor (βAR) antagonist propranolol at an effective dose (25, 26). LC projections to LA are ipsilateral (38), and therefore unilateral LC manipulations should not affect the contralateral LA. Indeed, simultaneous ipsilateral drug infusions in LC and LA had no effect on LTM (Fig. 5 *A* and *C*; one-way ANOVA and Tukey's multiple comparison test, vehicle vs. ipsilateral drug treatment, not significant), indicating that an intact unilateral LC-LA projection is sufficient for normal threat learning.

In contrast, contralateral drug-treated animals in which the circuit is disrupted in both hemispheres (at the level of LC on one side and LA on the other) displayed a significant decrease in LTM freezing compared with ipsilateral and contralateral vehicle-treated animals and ipsilateral drug-infused animals [Fig. 5 *B* and *C*; one-way ANOVA, $F(2,27) = 6.24$, $P = 0.006$, Tukey's multiple comparison test, contralateral drug treatment vs. vehicle, $P < 0.05$, contralateral drug treatment vs. ipsilateral drug treatment, $P < 0.05$]. These data indicate that that a functional hypothalamus (orexin)-LC-LA circuit is necessary for normal threat memory formation and that the orexin-to-LC projection enhances aversive learning by evoking norepinephrine release in the LA.

Discussion

Here we uncover a serial circuit between the hypothalamus, LC, and the amygdala and demonstrate that orexin activity in the LC acts as a key signal for emotional memory formation. Our data show that orexin fibers originating in the perifornical region of the hypothalamus directly depolarize LC neurons through rapid corelease of glutamate and orexin and that the orexin component, likely via activation of OrxR1, modulates downstream circuit elements to enhance threat conditioning. We also demonstrate

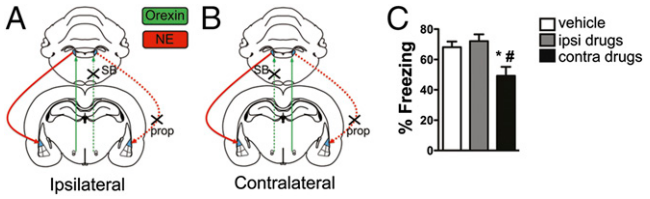

Fig. 5. A hypothalamus:LC:LA circuit mediated by orexin is required for threat conditioning. (*A* and *B*) Schematic of the disconnection strategy in which the OrxR1 antagonist SB 334867 (1 μg) is unilaterally infused into the LC, and the β-adrenergic receptor (βAR) antagonist propranolol hydrochloride (prop) was infused in the ipsilateral (*A*, control group) or contralateral (*B*, experimental group) LA. (*C*) Contralateral drug infusions, but not ipsilateral drug infusions or vehicle infusions, significantly reduced threat memory formation. Bar plots indicate mean ± SEM. $*P < 0.05$ relative to the ipsilateral drug infusion group, $^{\#}P < 0.05$ relative to the vehicle infusion group, one-way ANOVA followed by Tukey's multiple comparison test.

that orexin activity in the LC can drive norepinephrine signaling through βARs in the lateral nucleus of the amygdala to enhance threat memory formation.

Our finding of a critical role for orexin action in LC during threat conditioning complements previous reports showing that orexin neurons are activated in response to salient or arousing stimuli (38–40). Recent work using brief optical stimulation of orexin neurons provides functional evidence that orexin mediates sleep-to-wake transitions by activating LC neurons and that this modulation occurs through OrxR1 (40, 41). However, what does this mean in terms of the current results? In light of the work presented here, the orexin-to-LC circuit may represent a saliency signal that, in a natural context, arouses the animal during exposure to threatening or painful stimuli and primes neural circuits underlying threat conditioning. By increasing LC activity, OrxR1 signaling can increase norepinephrine release and induce activation of βARs in the amygdala, thereby enhancing plasticity in lateral amygdala neurons (27).

In slices, we demonstrate that optical stimulation of orexin fibers directly triggers both an AMPA receptor–mediated glutamatergic response, which is consistent with other findings (37), and an OrxR1-dependent depolarization in LC cells (5, 20, 21). Although synaptic glutamate release is likely critical for hypothalamus–LC communication, we show that OrxR1 activation is likely to play a key role by enhancing synaptic depolarization in LC cells.

Many neuromodulatory cells corelease both glutamate and a modulator. The modulatory component is often more subtle and prolonged, as is the case here, and is consistent with a volume transmission-type mechanism (42). The subtle, OrxR1-mediated depolarization that we observe in vitro could enhance synaptic summation and firing in LC cells in vivo, thereby increasing norepinephrine release in the LA. Consistent with this idea, previous work has shown that OrxA infusion into the LC triggers norepinephrine release and synaptic enhancement in the hippocampal dentate gyrus in vivo (43). A similar mechanism in the amygdala may be responsible for our behavioral results.

It is important to consider if orexin release in LC would, in the absence of a US, be sufficient to enhance memory formation. Threat conditioning is thought to occur by way of Hebbian processes in the amygdala, whereby the US strongly depolarizes LA neurons and alters synaptic transmission at coactive CS input synapses in the LA (28). Therefore, it is unlikely that BAR activation in the absence of an aversive stimulus would be sufficient for plasticity and learning.

Our results suggest that OrxR1 activity in LC during the learning episode is required for threat memory acquisition, although we cannot exclude the possibility that activation of OrxR1 also engages signaling cascades that may be required for later consolidation processes as has been suggested recently (44). A previous study demonstrated that βAR activation in LA enhances threat conditioning in a way that mirrors the effect of OrxR1 activity in LC; i.e., receptor activation is required during, but not following the learning episode (25). Together, these findings support a critical role for the hypothalamus:LC:LA circuit during the learning episode.

Our findings are consistent with studies in human orexin-compromised narcoleptics, who are impaired in acquiring a conditioned threat response and show reduced amygdala activity relative to controls when exposed to aversively conditioned stimuli (45, 46). This impairment is effectively the opposite of what is observed in disorders such as posttraumatic stress disorder (PTSD), which involves states of hyperarousal, a hyperactive amygdala, and the inability to control fear responses (47, 48). Indeed, cerbrospinal fluid (CSF) orexin levels are altered in patients with PTSD (49), as are norepinephrine levels (50), and a recent study in humans also showed that orexin-A levels in the amygdala positively correlate with emotional state (51). Dysregulation of the orexin system might explain susceptibility to PTSD or occur as a result of the disease, and thus might provide a specific target for treatment in these individuals. Orexin receptor antagonists have been used in clinical trials for other purposes (52), but OrxR1 antagonism may provide relief for chronic stress and related disorders.

In sum, the current work describes a unique circuit mechanism linking stress, arousal and threat learning mediated by the orexin system. Dysregulation of the orexin system or downstream noradrenergic mechanisms could serve as both a diagnostic measure and a treatment target for fear and anxiety disorders in susceptible individuals.

Materials and Methods

Detailed methods can be found in *SI Materials and Methods*.

Subjects. Adult male Sprague–Dawley rats were used. All procedures were conducted in accordance with the National Institutes of Health *Guide for the Care and Use of Experimental Animals* and were approved by the New York University Animal Care and Use Committee.

Stereotaxic Surgery. Procedures for stereotaxic surgery have been previously described (25). For amygdala experiments, cannulae were aimed at the LA; for ICV experiments, rats were implanted with single guide cannulae aimed at the right lateral ventricle; for LC experiments, double guide cannulae were aimed at LC; and for disconnection experiments, rats were implanted with one guide targeting the LC and the other targeting LA.

For optogenetic experiments, virus was unilaterally injected into the PFH. After 2–4 wk, animals were handled and subjected to behavioral conditioning or euthanized for slice physiology as described below.

Drug Preparation, Microinfusion, and Behavior. SB 334867 (Tocris) was prepared for three dose groups: 300 ng, 1.0 μg, or 5 μg/0.3 μL/side (5 μg/5 μL for ICV). TCS OX2 29 (Tocris) was used at 5 μg/5 μL ICV. For disconnection experiments propranolol (±propranolol hydrochloride; Sigma-Aldrich) was administered at 1 μg/0.3 μL. Rats were infused at 0.1 or 2.5 μL/min for ICV infusions and were allowed to move freely in their home cage during infusions. Afterward, cannulae were left in place for an additional 1–2 min to allow drug diffusion away from the cannula tip. For all experiments, animals were infused only once (no within-subject experiments were performed). Animals were handled 1 d before training to minimize the stress of infusion. Drug infusions occurred 15–20 min before training, immediately after training (for testing consolidation), or 15–20 min before expression test. For disconnection experiments, propranolol was infused into LA simultaneously with SB 334867 infusion in LC. Vehicle-infused controls were included for both contralateral and ipsilateral animals and were combined for analysis due to no significant difference between groups ($P = 0.77$). Freezing data were scored offline and analyzed using GraphPad Prism (GraphPad Software).

Channelrhodopsin Experiments. Procedures are as described previously (36). Orexin neuron-specific lentivirus constructs pLV-Hcrt::ChR2-mCherry and pLV-Hcrt:: mCherry have been described (34), and were produced by the University of North Carolina Gene Therapy Center (Vector Core Services). Before training, a fiber optic cable was inserted ∼0.5 mm above the dorsal tip of the LC. A three CS–US pairing protocol was used where each CS consisted of a series of auditory pips and the US was blue light laser stimulation combined with a weak, ∼0.5-mA footshock that coterminated with the last 2 s of the CS. A weak training protocol was used to obtain lower baseline freezing levels (∼50%) and thus avoid ceiling effects on freezing levels. In another set of ChR2-expressing animals, pretraining infusion of SB 334867 (1 μg/0.3 μg) or vehicle preceded conditioning by 20 min. Twenty-four hours following training, animals were placed in a novel context (same LTM context as all other experiments), and following a 3-min acclimation period, animals were presented with five CSs at a random intertrial interval no longer than 5 min.

For c-Fos detection, animals were handled for 3 d before light stimulation to reduce baseline c-Fos levels. Ninety minutes following stimulation, animals were perfused for histological processing.

Histology and Immunohistochemistry. Histology for cannula targeting was performed as described previously (25). To verify targeting area and cell specificity of viral expression, neuronal activity in the LC immunohistochemistry was performed to detect mCherry (1:500; Clontech Laboratories), orexin-A (1:500; R&D Systems), c-Fos (1:5,000; Calbiochem), and DBH (1:2,000; EMD).

Slice Preparation, Whole-Cell Recordings, and Data Acquisition. We prepared 260- to 280-μm-thick acute coronal slices of hypothalamus and horizontal slices containing LC from adult rats. Animals were anesthetized and transcardially perfused with ice-cold oxygenated slicing solution. Brains were removed immediately and immersed in ice-cold, oxygenated slicing solution. Slices were prepared, transferred to a 32–33 °C chamber, and maintained in continuously oxygenated artificial CSF (aCSF). After 30–45 min, slices were kept at room temperature and until recording at 32 ± 0.5 °C.

Whole-cell current clamp recordings were conducted in orexin projection cells of the medial PFH (identified by fluorescence) or from principal cells of the LC. Photo-activation in slices was achieved using a 470-nm high-power LED (Thorlabs) coupled to the microscope using a customized Siskiyou beamsplitter cube. Data were acquired and analyzed using PClamp software (Molecular Devices). Signals were acquired using an AxoClamp 2B amplifier, digitized through a Digidata 1440A at a sampling rate of 25 kHz, and filtered online at 10 kHz. We conducted statistical analyses in Matlab (Mathworks) using standard resampling methods, including the Matlab Resampling Package.

ACKNOWLEDGMENTS. We thank M. Hou, B. T. Elie, and E. C. Andrade for technical assistance and C. K. Cain for editing the manuscript. Research reported in this publication was supported by National Institutes of Health Award F32MH094062.

1. Hess WR, Akert K (1955) Experimental data on role of hypothalamus in mechanism of emotional behavior. *AMA Arch Neurol Psychiatry* 73(2):127–129.
2. Nakao H (1958) Emotional behavior produced by hypothalamic stimulation. *Am J Physiol* 194(2):411–418.
3. de Lecea L, et al. (1998) The hypocretins: Hypothalamus-specific peptides with neuroexcitatory activity. *Proc Natl Acad Sci USA* 95(1):322–327.
4. Sakurai T, et al. (1998) Orexins and orexin receptors: A family of hypothalamic neuropeptides and G protein-coupled receptors that regulate feeding behavior. *Cell* 92(4):573–585.
5. Ivanov A, Aston-Jones G (2000) Hypocretin/orexin depolarizes and decreases potassium conductance in locus coeruleus neurons. *Neuroreport* 11(8):1755–1758.
6. Borgland SL, Storm E, Bonci A (2008) Orexin B/hypocretin 2 increases glutamatergic transmission to ventral tegmental area neurons. *Eur J Neurosci* 28(8):1545–1556.
7. Winsky-Sommerer R, Boutrel B, de Lecea L (2005) Stress and arousal: The corticotrophin-releasing factor/hypocretin circuitry. *Mol Neurobiol* 32(3):285–294.
8. Aston-Jones G (2005) Brain structures and receptors involved in alertness. *Sleep Med* 6 (Suppl 1):S3–S7.
9. Aston-Jones G, et al. (2010) Lateral hypothalamic orexin/hypocretin neurons: A role in reward-seeking and addiction. *Brain Res* 1314:74–90.
10. Marcus JN, et al. (2001) Differential expression of orexin receptors 1 and 2 in the rat brain. *J Comp Neurol* 435(1):6–25.
11. Wu MF, Nienhuis R, Maidment N, Lam HA, Siegel JM (2011) Role of the hypocretin (orexin) receptor 2 (Hcrt-r2) in the regulation of hypocretin level and cataplexy. *J Neurosci* 31(17):6305–6310.
12. Mang GM, et al. (2012) The dual orexin receptor antagonist almorexant induces sleep and decreases orexin-induced locomotion by blocking orexin 2 receptors. *Sleep* 35(12):1625–1635.
13. Harris GC, Wimmer M, Aston-Jones G (2005) A role for lateral hypothalamic orexin neurons in reward seeking. *Nature* 437(7058):556–559.
14. Smith RJ, See RE, Aston-Jones G (2009) Orexin/hypocretin signaling at the orexin 1 receptor regulates cue-elicited cocaine-seeking. *Eur J Neurosci* 30(3):493–503.
15. Johnson PL, et al. (2012) Activation of the orexin 1 receptor is a critical component of CO2-mediated anxiety and hypertension but not bradycardia. *Neuropsychopharmacology* 37(8):1911–1922.
16. Lungwitz EA, et al. (2012) Orexin-A induces anxiety-like behavior through interactions with glutamatergic receptors in the bed nucleus of the stria terminalis of rats. *Physiol Behav* 107(5):726–732.
17. Furlong TM, Vianna DM, Liu L, Carrive P (2009) Hypocretin/orexin contributes to the expression of some but not all forms of stress and arousal. *Eur J Neurosci* 30(8): 1603–1614.
18. Steiner MA, Lecourt H, Jenck F (2012) The brain orexin system and almorexant in fear-conditioned startle reactions in the rat. *Psychopharmacology (Berl)* 223(4):465–475.
19. van den Pol AN, et al. (2002) Hypocretin (orexin) enhances neuron activity and cell synchrony in developing mouse GFP-expressing locus coeruleus. *J Physiol* 541(Pt 1): 169–185.
20. Horvath TL, et al. (1999) Hypocretin (orexin) activation and synaptic innervation of the locus coeruleus noradrenergic system. *J Comp Neurol* 415(2):145–159.
21. Soffin EM, et al. (2002) SB-334867-A antagonises orexin mediated excitation in the locus coeruleus. *Neuropharmacology* 42(1):127–133.
22. Mileykovskiy BY, Kiyashchenko LI, Siegel JM (2005) Behavioral correlates of activity in identified hypocretin/orexin neurons. *Neuron* 46(5):787–798.
23. Chen FJ, Sara SJ (2007) Locus coeruleus activation by foot shock or electrical stimulation inhibits amygdala neurons. *Neuroscience* 144(2):472–481.
24. Winsky-Sommerer R, et al. (2004) Interaction between the corticotropin-releasing factor system and hypocretins (orexins): A novel circuit mediating stress response. *J Neurosci* 24(50):11439–11448.
25. Bush DE, Caparosa EM, Gekker A, Ledoux J (2010) Beta-adrenergic receptors in the lateral nucleus of the amygdala contribute to the acquisition but not the consolidation of auditory fear conditioning. *Front Behav Neurosci* 4:154.
26. Debiec J, Ledoux JE (2004) Disruption of reconsolidation but not consolidation of auditory fear conditioning by noradrenergic blockade in the amygdala. *Neuroscience* 129(2):267–272.
27. Tully K, Bolshakov VY (2010) Emotional enhancement of memory: How norepinephrine enables synaptic plasticity. *Mol Brain* 3:15.
28. LeDoux JE (2000) Emotion circuits in the brain. *Annu Rev Neurosci* 23:155–184.
29. Fanselow MS (1980) Conditioned and unconditional components of post-shock freezing. *Pavlov J Biol Sci* 15(4):177–182.
30. Huang SC, Dai YW, Lee YH, Chiou LC, Hwang LL (2010) Orexins depolarize rostral ventrolateral medulla neurons and increase arterial pressure and heart rate in rats mainly via orexin 2 receptors. *J Pharmacol Exp Ther* 334(2):522–529.
31. Peyron C, et al. (1998) Neurons containing hypocretin (orexin) project to multiple neuronal systems. *J Neurosci* 18(23):9996–10015.
32. Lee HJ, Berger SY, Stiedl O, Spiess J, Kim JJ (2001) Post-training injections of catecholaminergic drugs do not modulate fear conditioning in rats and mice. *Neurosci Lett* 303(2):123–126.
33. Schafe GE, LeDoux JE (2000) Memory consolidation of auditory pavlovian fear conditioning requires protein synthesis and protein kinase A in the amygdala. *J Neurosci* 20(18):RC96.
34. Adamantidis AR, Zhang F, Aravanis AM, Deisseroth K, de Lecea L (2007) Neural substrates of awakening probed with optogenetic control of hypocretin neurons. *Nature* 450(7168):420–424.
35. Johnson PL, et al. (2010) A key role for orexin in panic anxiety. *Nat Med* 16(1): 111–115.
36. Johansen JP, et al. (2010) Optical activation of lateral amygdala pyramidal cells instructs associative fear learning. *Proc Natl Acad Sci USA* 107(28):12692–12697.
37. Schöne C, et al. (2012) Optogenetic probing of fast glutamatergic transmission from hypocretin/orexin to histamine neurons in situ. *J Neurosci* 32(36):12437–12443.
38. Jones BE, Moore RY (1977) Ascending projections of the locus coeruleus in the rat. II. Autoradiographic study. *Brain Res* 127(1):25–53.
39. Gompf HS, Aston-Jones G (2008) Role of orexin input in the diurnal rhythm of locus coeruleus impulse activity. *Brain Res* 1224:43–52.
40. Carter ME, et al. (2010) Tuning arousal with optogenetic modulation of locus coeruleus neurons. *Nat Neurosci* 13(12):1526–1533.
41. Adamantidis A, Carter MC, de Lecea L (2010) Optogenetic deconstruction of sleep-wake circuitry in the brain. *Front Mol Neurosci* 2:31.
42. Rice ME, Cragg SJ (2008) Dopamine spillover after quantal release: Rethinking dopamine transmission in the nigrostriatal pathway. *Brain Res Brain Res Rev* 58(2): 303–313.
43. Walling SG, Nutt DJ, Lalies MD, Harley CW (2004) Orexin-A infusion in the locus ceruleus triggers norepinephrine (NE) release and NE-induced long-term potentiation in the dentate gyrus. *J Neurosci* 24(34):7421–7426.
44. Soya S, et al. (2013) Orexin receptor-1 in the locus coeruleus plays an important role in cue-dependent fear memory consolidation. *J Neurosci* 33(36):14549–14557.
45. Khatami R, Birkmann S, Bassetti CL (2007) Amygdala dysfunction in narcolepsy-cataplexy. *J Sleep Res* 16(2):226–229.
46. Ponz A, et al. (2010) Reduced amygdala activity during aversive conditioning in human narcolepsy. *Ann Neurol* 67(3):394–398.
47. Milad MR, et al. (2009) Neurobiological basis of failure to recall extinction memory in posttraumatic stress disorder. *Biol Psychiatry* 66(12):1075–1082.
48. Jovanovic T, Ressler KJ (2010) How the neurocircuitry and genetics of fear inhibition may inform our understanding of PTSD. *Am J Psychiatry* 167(6):648–662.
49. Strawn JR, Geracioti TD, Jr. (2008) Noradrenergic dysfunction and the psychopharmacology of posttraumatic stress disorder. *Depress Anxiety* 25(3):260–271.
50. Geracioti TD, Jr., et al. (2001) CSF norepinephrine concentrations in posttraumatic stress disorder. *Am J Psychiatry* 158(8):1227–1230.
51. Blouin AM, et al. (2013) Human hypocretin and melanin-concentrating hormone levels are linked to emotion and social interaction. *Nat Commun* 4:1547.
52. Coleman PJ, Renger JJ (2010) Orexin receptor antagonists: a review of promising compounds patented since 2006. *Expert Opin Ther Pat* 20(3):307–324.

Supporting Information

Sears et al. 10.1073/pnas.1320325110

SI Materials and Methods

Subjects. Adult male Sprague–Dawley rats, weighing 250–275 g on arrival, were obtained from Hilltop Laboratory. Animals were allowed at least 1–2 wk of acclimation to the vivarium before surgeries. Rats were individually housed in transparent plastic high-efficiency particulate absorption (HEPA)-filtered cages and maintained on a 12/12-h light/dark cycle (lights on at 0700 hours) within a temperature- and humidity-controlled environment. Food and water were available ad libitum throughout the duration of the experiments. All experiments were conducted during the light cycle. All procedures were conducted in accordance with the National Institutes of Health *Guide for the Care and Use of Experimental Animals* and were approved by the New York University Animal Care and Use Committee.

Stereotaxic Surgery. Rats were anesthetized with a mixture of ketamine (100 mg/kg, i.p.) and xylazine (10 mg/kg, i.p.), with supplementation as needed, along with buprenorphine–HCl (0.02 mg/kg, s.c.) for analgesia, and placed in a stereotaxic apparatus (David Kopf Instruments). Brain areas were targeted using coordinates (1). For behavioral pharmacology experiments, stainless steel guide cannulae (22 gauge; Plastics One) were lowered into position and secured to the skull using surgical screws and acrylic dental cement (Ortho-jet; Lang Dental Manufacturing Co.). Twenty-eight gauge dummy cannulae, cut to extend 0.5 mm from the guides, were inserted to prevent clogging. For amygdala experiments, cannulae were aimed at the lateral amygdala (LA) [from bregma: anterior/posterior (AP) −3.2; medial/lateral (ML) ± 5.3; dorsal/ventral (DV) −6.5 from skull for infusion 1.5 mm below the guide]. For intracerebroventricular (ICV) experiments, rats were implanted with single guide cannulae aimed at the right lateral ventricle (from bregma: AP −0.8; ML + 1.5; DV −3.4 from skull) for infusion 0.5 mm below the guide. For locus coeruelus (LC) experiments, double guide cannulae were used (from lambda: AP −0.8; ML ± 1.3, DV −5.3) for infusion 2 mm beyond guides. For pharmacological disconnection experiments, rats were implanted with one guide targeting the LC (from lambda: AP −0.8; ML +1.3, DV −5.3; 2-mm extension for infusion) and the other targeting LA (from bregma: AP −3.2; ML ± 5.4; DV −6.5 from skull; 1.5-mm extension for infusion). After surgery, rats were administered buprenorphine hydrochloride (0.02 mg/kg, s.c.) for analgesia and given 7–10 d to recover from surgery before behavioral manipulations.

For optogenetic experiments, virus was unilaterally injected into the perifornical hypothalamus (from bregma: AP −3.12; ML ± 1.3, DV −8.7) to a volume of 1 μL using a 10-μL Gastight Hamilton syringe (Hamilton Company) at a rate of 0.1 μL/min. Following viral infusion, a 20-gauge guide cannula was lowered to a position ∼2 mm above the LC (from lambda: AP −0.8; ML ± 1.3, DV −5.3) and secured to the skull using surgical screws and dental cement. Animals remained under quarantine in the BSL2 facility for 48 h following surgeries, after which they were returned to the vivarium. After 2–4 wk to allow for lentivirus infection and expression, animals were handled and subjected to behavioral conditioning or killed for slice physiology as described below.

Drug Preparation and Microinfusion. SB 334867 was obtained from Tocris and dissolved in 25% (wt/vol) β-cyclodextrin and 5–10% (vol/vol) DMSO in artificial cerebrospinal fluid (aCSF: 25 mM D-glucose, 115 mM NaCl, 24 mM Na_2PO_4, 3.3 mM KCl, 2 mM $CaCl_2$, 1 mM $MgSO_4$, 25.5 mM $NaHCO_3$; pH 7.4) or 0.9% sterile saline. Concentrations were prepared for three dose groups: 0, 300 ng, 1.0 μg, or 5 μg/0.3 μL/side (5 μg/5 μL for ICV). TCS OX2 29 was obtained from Tocris and used at 5 μg/5 μL ICV in aCSF. For disconnection experiments, propranolol (± propranolol hydrochloride; Sigma-Aldrich) was dissolved in 0.9% sterile saline and administered at 1 μg/0.3 μL as in our previous study (2). For the drug infusions, internal infusion cannulae were attached to 10-μL Hamilton syringes via 0.015 × 0.043 × 0.014-in. polyethylene tubing obtained from A-M Systems. Tubing and syringes were backfilled with distilled water, and a small air bubble separated the water from the infusate. Rats were infused using an infusion pump (PHD 2000; Harvard Apparatus) that delivered drug at a constant rate of 0.1 μL/min for direct infusions or 2.5 μL/min for ICV infusions. Animals were allowed to move freely in their home cage during infusions. After infusion was complete, cannulae were left in place for an additional 1–2 min to allow drug diffusion away from the cannula tip. Following all ICV experiments, angiotensin II (50 ng/5 μL; Tocris) was infused to assess targeting. Only animals showing a rapid drinking response following infusion were included in the analysis (3).

Apparatus. For pharmacology experiments, rats underwent fear conditioning in 1 of 10 identical chambers (Rat Test Cage; Coulbourn Instruments) constructed of aluminum and Plexiglas walls, with metal stainless steel rod flooring that was attached to a shock generator (Model H13-15; Coulbourn Instruments). The chambers were lit with a single house light, and each chamber was enclosed within a sound isolation cubicle (Model H10-24A; Coulbourn Instruments). Long-term memory testing took place within a modified version of the context, with smooth black plastic flooring, mild peppermint scent, and a striped pattern on the Plexiglas door. An infrared digital camera, mounted on top of each chamber, allowed videotaping during behavioral procedures for subsequent behavioral scoring. A computer, installed with Graphic State 2 software and connected to the chambers via the Habitest Linc System (Coulbourn Instruments), controlled the presentation of stimuli during behavioral sessions. Apparati and procedures were slightly different for optogenetic experiments and are described in detail in a previous publication (4). Briefly, animals were trained in Med-Associates boxes without a houselight. All other conditions were similar to those described above.

Behavioral Pharmacology Procedures. Animals were allowed at least 1 wk of recovery following surgery. Animals were handled 1 d before training to minimize the stress of infusion. Drug infusions occurred 15–20 min before training, immediately after training (for testing consolidation) or 15–20 min before expression test. For disconnection experiments, propranolol was infused into LA simultaneously with SB 334867 infusion in LC. Vehicle-infused controls were included for both contralateral and ipsilateral animals and were combined for analysis due to no significant difference between groups ($P = 0.77$). Following infusion, cannulae were left in place for 1 min to allow for drug diffusion into the tissue. Conditioning procedures have been used extensively by our laboratory, and specific methods are detailed in available publications (5, 6). Briefly, following a 5-min acclimation period, animals received three conditioned stimulus (CS)–unconditioned stimulus (US) pairing in which the CS is a 30-s presentation of a 5-kHz, 80-db tone and the US is a standard, 1-s coterminating footshock (0.6 mA for ICV experiments, 0.7 mA for LC and LA experiments). Following training, animals were returned to their

home cage. Chamber floors, trays, and walls were thoroughly cleaned with water and dried between sessions. Twenty-four hours following training, animals were tested in a separate context (see Apparatus section) for long-term memory (LTM) (7). LTM test consisted of five CS presentations, and freezing time was quantified offline to assess threat (freezing) levels. Freezing behavior was blindly scored by an investigator and in some cases verified by other investigators. Data are presented as the mean percent of time freezing during all CS presentations. After experiments, animals were perfused with 10% formalin, and cannulae targeting was histologically verified as described (5, 6).

To confirm that our results were not due to shock reactivity in the LC or nearby sites, we assessed responses to increasing shock intensity following antagonism of OrxR1 in LC (8) (Fig. S1). For this experiment, 10 footshocks were delivered with increasing intensity (0.1–1 mA), each 1 s in duration with 30 s separating each trial. For quantification, responses to increasing shock intensity were assigned arbitrary numbers: 0 = unnoticed, 1 = noticed, 2 = flinch, and 3 = jump.

Channelrhodopsin Experiments. Procedures were similar to experiments described in a previous publication (4). The orexin neuron–specific lentivirus constructs pLV-Hcrt::ChR2-mCherry and pLV-Hcrt:: mCherry were generously provided by Luis De Lecea (Stanford University, Stanford, CA) (9), and the virus produced by the University of North Carolina Gene Therapy Center (Vector Core Services, Chapel Hill, NC). This virus effectively targets orexin neurons in rats (Fig. 4). Animals expressing a reporter virus (Hcrt::mCherry) controlled for channelrhodopsin (ChR) expression effects and animals expressing Hcrt::ChR-mCherry (with no light presentation) controlled for possible blue light effects. Animals were allowed 3–4 wk recovery following viral infusion and cannulation to allow for sufficient expression. Before training, a fiber optic cable (200 μm core diameter, 0.37 numerical aperture) fed through a cannula connector assembly (Plastics One) was inserted into the guide cannulae and extended 1.3–1.5 mm beyond the tip of the guide, placing the fiber ∼0.5 mm above the dorsal tip of the LC. The cable and connector assembly were painted with black nail polish or covered with black electrical tape to avoid possible conditioning effects to the flashing blue light. The fiber optic cable was attached to a 473-diode pumped solid-state laser (Laserglow Technologies), which output 20–30 mW from the tip of the fiber optic cable. A three CS–US pairing protocol was used where each CS consisted of a series of auditory pips (5-kHz tone pips at 1 Hz with 250 ms on and 750 ms off for 20 s) and the US was blue light laser stimulation (470-nm laser, 20 Hz, 10-ms pulse durations) combined with a weak, ∼0.5-mA footshock that coterminated with the last 2 s of the CS (4). Each trial was separated by a random intertrial interval (2–5 min). A weak training protocol was used to obtain lower baseline freezing levels (∼50%) and thus avoid ceiling effects on freezing levels. In another set of Hcrt::ChR2-mCherry–expressing animals, pretraining infusion of the OrxR1 antagonist SB 334867 (1 μg/0.3 μg) or vehicle preceded conditioning by 20 min. Twenty-four hours following training, animals were placed in a novel context (Apparatus section), and following a 3-min acclimation period, animals were exposed to five CSs (5-kHz tone pips at 1 Hz with 250 ms on and 750 ms off for 20 s) with a random intertrial interval no longer than 5 min.

Procedures for c-Fos detection are similar to our previous study (4). Briefly, animals were handled for 3 d before light stimulation to reduce baseline c-Fos levels. Ninety minutes following stimulation, animals were perfused as described below for histological processing.

Histology and Immunohistochemistry. Following behavior experiments, animals were overdosed with 25% chloral hydrate and transcardially perfused with either 10% formalin for histology to assess cannula placement or 4% paraformaldehyde in 0.01 M PBS for immunohistochemistry. Tissue processed for cannula placement was postfixed in 10% formalin or 4% paraformaldehyde at 4 °C until prepared for histological staining. For immunohistochemical processing, tissue was cryoprotected in a 30% sucrose–4% paraformaldehyde solution (in 0.01 M PBS) at 4 °C for at least 1 d and then stored in 0.01 M PBS. Brains were blocked coronally and cut on a freezing microtome. For histological verification of cannula targeting, tissue was cut at a thickness of 50 μm and kept in 0.01 M PBS until mounted on gelatin-coated slides and dried overnight. After standard histological Nissl staining and coverslipping, sections were examined on a light microscope for injector tip localization into LC or LA. Only data from rats with bilateral injector placements localized to the LC and LA were included in the study.

For immunohistochemistry, tissue was cut at 35 μm. Before antibody incubation, floating tissue was rinsed with agitation three times in 0.01 M PBS and blocked in 1% BSA in 0.01 M PBS for 1 h at room temperature. Immunohistochemical detection was achieved in primary antibody solutions containing 1% BSA, 0.2% Triton-X 100, and 0.02% NaAz. Sections were incubated overnight at room temperature in rabbit anti-dsRed (for detection of mCherry; 1:500; Clontech Laboratories) (10) and mouse anti–orexin-A (1:500; R&D Systems) antibodies for verification of targeting area and cell specificity of viral expression (11). For c-Fos experiments, LC sections were incubated in mouse anti-dopamine beta hydroxylase (DBH) (1:2,000; EMD Millipore) (12) and rabbit anti–c-Fos (1:5,000; Calbiochem) (13). Following primary antibody incubation, sections were rinsed with agitation three times for 5 min in 0.01 M PBS and incubated in Alexa-488 or -594 secondary antibody (Invitrogen) in 0.01 M PBS. Sections were rinsed three times for 5 min in PBS, mounted on gelatin-coated slides, and allowed to dry for several hours, followed by a brief wash in ddH_2O to remove excess salt (PBS), coverslipped in aqueous mount (ProLong Gold Antifade Reagent; Invitrogen), and allowed to cure overnight at room temperature before fluorescence imaging. For all experiments, animals were excluded from analysis if virus or cannulae targeting was outside the areas of interest.

Slice Preparation and Whole-Cell Recordings. We prepared 260- to 280-μm-thick acute coronal slices including the hypothalamus and 260- to 280-μm-thick horizontal brainstem slices including the LC from adult rats (>7 wk of age) expressing either the ChR2 construct or mCherry in orexinergic cells as described above. For LC experiments, we prepared acute horizontal brainstem slices to maximize synaptic connectivity between incoming fibers and dendritic arborizations of the LC cells. Slices were made at least 4 wk after injection of the virus to ensure adequate expression of ChR2 in axonal fibers for photoactivation within the slice preparation. Because the LC is a small structure, reliable responses could be obtained from only one high-quality slice per preparation. Although the amplitude of maximal depolarization varied from slice to slice, all four cells showed similar glutamatergic and orexinergic contributions to the fast and slow components of light-evoked synaptic responses. Animals were deeply anesthetized with 75–100 mg/kg ketamine + 10 mg/kg xylazine, and after confirmation of anesthesia, were transcardially perfused with ice-cold (4 °C) oxygenated slicing solution containing (in mM): 85 NaCl, 2.5 KCl, 1.2 NaH_2PO_4, 25 $NaHCO_3$, 7 $MgSO_4$, 0.5 $CaCl_2$, 25 glucose, and 75 sucrose. Animals were decapitated, and their brains removed immediately after perfusion, and brains were immersed in the same ice-cold slicing solution continuously bubbled with carbogen (95% O_2 and 5% CO_2). After at least 5 min, the portions of the brain containing the hypothalamus and LC were blocked separately. One area was sliced at a time, whereas the other was maintained

in oxygenated ice-cold slicing solution, and slices were prepared using an OTS-5000 tissue slicer (Electron Microscopy Sciences). Slices were then transferred to a heated chamber (32–33 °C) and maintained submerged in a continuously oxygenated aCSF containing (in mM) 125 NaCl, 3.3 KCl, 1.2 NaH_2PO_4, 25 $NaHCO_3$, 1.2 $MgSO_4$, 2 $CaCl_2$, 15 glucose, 0.01 D-serine, and 0.5 ascorbic acid. Slices were maintained at the heated temperature for 30–45 min and then kept at room temperature. We conducted all recordings at 32 ± 0.5 °C in the same aCSF used to maintain slices.

Whole-cell current clamp recordings were conducted in orexinergic projection cells of the dorsomedial hypothalamus (identified by fluorescence) or from principal cells of the LC on an upright Olympus BX51-W1 microscope. The LC was readily identified under IR-DIC imaging as a lucid area near the fourth ventricle containing large, densely packed cell bodies (14, 15). All recordings were obtained using 4- to 7-MΩ borosilicate glass pipettes filled with an internal solution containing (in mM) 136 potassium gluconate, 4 $MgCl_2$, 1 EGTA, 0.1 $CaCl_2$, 4 Na-ATP, 0.3 Na-GTP, 10 Hepes, and 15 μM Alexa Fluor-594 (pH 7.3; 291 mOsm). Orexinergic projection cells in the dorsomedial hypothalamus exhibited spontaneous firing and a resting membrane potential of approximately −50 mV and were held at −60 mV. Noradrenergic cells of the LC were characterized by low-frequency spontaneous firing (16, 17) and a depolarized resting membrane potential (approximately −45 mV) and were held at −55 mV. Reported potentials are uncorrected for a calculated liquid junction potential of 13 mV (PClamp Liquid Junction Calculator).

Photoactivation in acute slices was achieved using a 470-nm mounted high-power LED (Thorlabs) coupled to the microscope using a customized Siskiyou beamsplitter cube containing a sliding mirror to bring the LED beam in and out of the light path. Maximal light power was calculated as 4 mW after the 40× objective used for all recordings. For optically elicited synaptic responses in the LC, we delivered a 500-ms, 20-Hz train of light stimulation (10-ms pulse duration) every 30 s, interleaved with sweeps where no light was delivered. Values in baseline and drug conditions were calculated based on the average of the last five sweeps in each condition.

Data Acquisition for Slice Physiology. All electrophysiological data were acquired and analyzed using PClamp software (Molecular Devices). Signals were acquired using an AxoClamp 2B amplifier, digitized through a Digidata 1440A at a sampling rate of 25 kHz, and filtered online at 10 kHz. The fast component of light-activated transmission onto LC cells was measured as the maximal amplitude of the first excitatory postsynaptic potential (EPSP), measured in the initial 50 ms after the first light onset of a train. The slower component of light-activated depolarization onto LC cells was measured as the area under the response, in a window beginning at EPSP onset and ending 700 ms later. We conducted statistical analyses in Matlab (Mathworks) using standard resampling methods, including the commercially available Matlab Resampling Package.

Statistical Analysis. All data used in parametric tests were plotted and visually found to be compatible with the assumption of normal distribution. For behavioral data, a Student t test was used to analyze freezing levels when comparing two groups of averaged data, and one-way ANOVA was used for comparing more than one group followed by a Tukey's multiple comparison test. Bartlett's test for equal variances was used for one-way ANOVAs (18), whereas the F test was used for the Student t test to confirm that variances were not significantly different in compared groups (GraphPad Software). To analyze US sensitivity data, a repeated-measures ANOVA was used to compare freezing between vehicle and drug-treated groups and was followed by Bonferonni post hoc tests. Error bars in all figures represent ±SEM. Data were analyzed using GraphPad Prism.

For c-Fos experiments, to meet the assumption of equal variance across groups, the data were transformed using the equation $Y = \log(X + 1)$. A two-way ANOVA was subsequently used, followed by the Bonferonni posttest.

For electrophysiology experiments, we performed one-way ANOVAs and paired comparisons using resampling methods. Resampling was used because of the low sample size and inequality of variance due to low slice yield per animal and was intended to minimize the number of animals required for the experiment. Briefly, an F-statistic was calculated from the experimental data for the variable of interest, using the absolute value of the sum of errors. All data were then pooled and used to generate randomized data sets (100,000 iterations).

1. Paxinos G, Watson C (1998) *The Rat Brain in Stereotaxic Coordinates* (Academic Press, San Diego), 4th Ed.
2. Bush DE, Caparosa EM, Gekker A, Ledoux J (2010) Beta-adrenergic receptors in the lateral nucleus of the amygdala contribute to the acquisition but not the consolidation of auditory fear conditioning. *Front Behav Neurosci* 4:154.
3. Houpt TA, Corp ES, Berlin R (1998) Intracerebroventricular angiotensin II increases intraoral intake of water in rats. *Peptides* 19(1):171–173.
4. Johansen JP, et al. (2010) Optical activation of lateral amygdala pyramidal cells instructs associative fear learning. *Proc Natl Acad Sci USA* 107(28):12692–12697.
5. Debiec J, Ledoux JE (2004) Disruption of reconsolidation but not consolidation of auditory fear conditioning by noradrenergic blockade in the amygdala. *Neuroscience* 129(2):267–272.
6. Schafe GE, et al. (2005) Memory consolidation of Pavlovian fear conditioning requires nitric oxide signaling in the lateral amygdala. *Eur J Neurosci* 22(1):201–211.
7. Schafe GE, LeDoux JE (2000) Memory consolidation of auditory pavlovian fear conditioning requires protein synthesis and protein kinase A in the amygdala. *J Neurosci* 20(18):RC96.
8. Morgan MA, LeDoux JE (1995) Differential contribution of dorsal and ventral medial prefrontal cortex to the acquisition and extinction of conditioned fear in rats. *Behav Neurosci* 109(4):681–688.
9. Adamantidis AR, Zhang F, Aravanis AM, Deisseroth K, de Lecea L (2007) Neural substrates of awakening probed with optogenetic control of hypocretin neurons. *Nature* 450(7168):420–424.
10. Adamantidis A, Carter MC, de Lecea L (2010) Optogenetic deconstruction of sleep-wake circuitry in the brain. *Front Mol Neurosci* 2:31.
11. Zhu Y, et al. (2007) Selective loss of catecholaminergic wake active neurons in a murine sleep apnea model. *J Neurosci* 27(37):10060–10071.
12. Farb CR, Chang W, Ledoux JE (2010) Ultrastructural characterization of noradrenergic axons and beta-adrenergic receptors in the lateral nucleus of the amygdala. *Front Behav Neurosci* 4:162.
13. Martinez RC, et al. (2013) Active vs. reactive threat responding is associated with differential c-Fos expression in specific regions of amygdala and prefrontal cortex. *Learn Mem* 20(8):446–452.
14. Banghart MR, Sabatini BL (2012) Photoactivatable neuropeptides for spatiotemporally precise delivery of opioids in neural tissue. *Neuron* 73(2):249–259.
15. Jüngling K, et al. (2012) Activation of neuropeptide S-expressing neurons in the locus coeruleus by corticotropin-releasing factor. *J Physiol* 590(Pt 16):3701–3717.
16. Alreja M, Aghajanian GK (1995) Use of the whole-cell patch-clamp method in studies on the role of cAMP in regulating the spontaneous firing of locus coeruleus neurons. *J Neurosci Methods* 59(1):67–75.
17. Hagan JJ, et al. (1999) Orexin A activates locus coeruleus cell firing and increases arousal in the rat. *Proc Natl Acad Sci USA* 96(19):10911–10916.
18. Snedecor GW, Cochran WG (1989) *Statistical Methods* (Iowa State Univ Press, Ames, IA), 8th Ed.

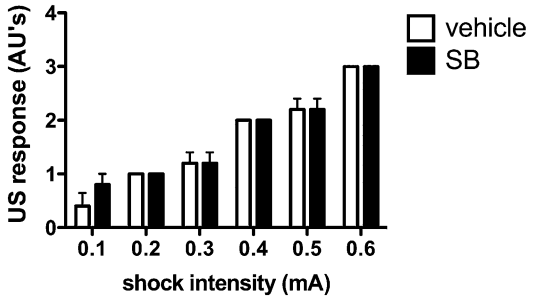

Fig. S1. SB 334867 in LC does not influence shock sensitivity. Amplitude was increased by 0.1 mA every 30 s from 0.1 to 1 mA. Responses were maximal by 0.6 mA [n = 5/group, two-way repeated-measures ANOVA; no significant interaction, $F(5,40) = 0.678$, $P = 0.64$; no main effect for drug treatment, $F(1,40) = 0.421$, $P = 0.53$; main effect of shock intensity, $F(5,40) = 80.81$, $P < 0.001$].

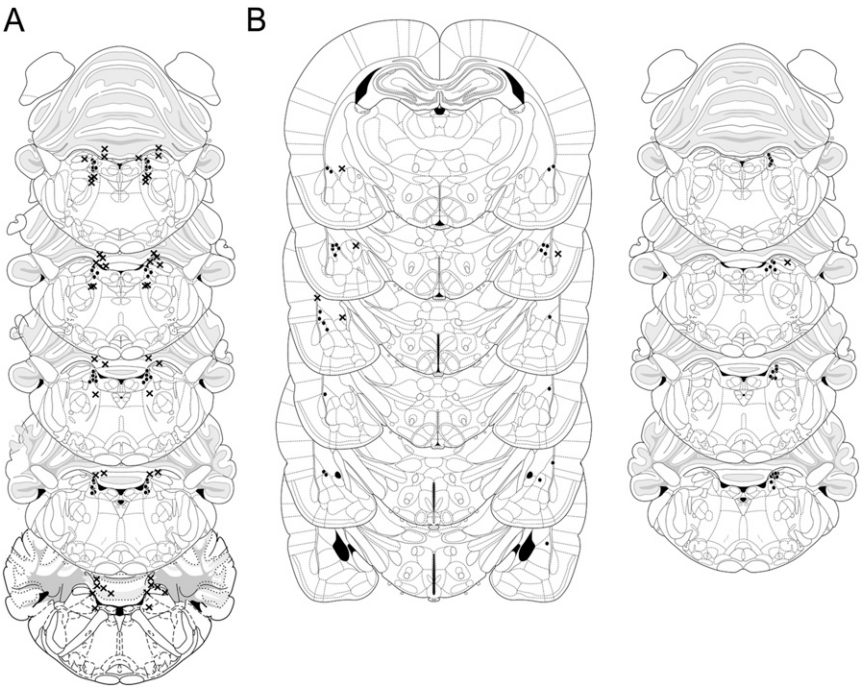

Fig. S2. Coronal rat sections depicting cannulae placement for microinfusion experiments. (*A*) Placements for bilateral LC infusion experiments. (*B*) Placements for disconnection experiments. Hits are denoted as black circles; misses are demarcated with an X.

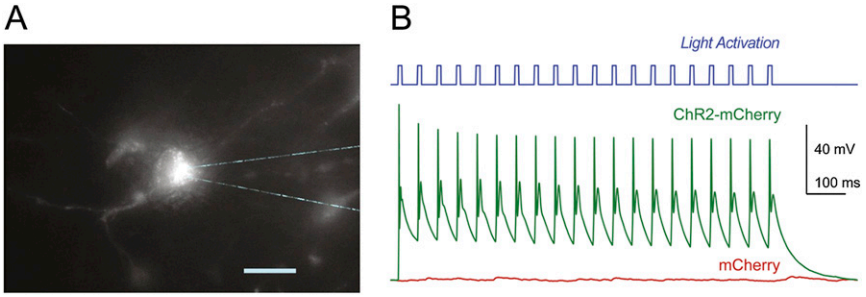

Fig. S3. Blue light activates neurons expressing ChR2. (*A*) Wide-field fluorescent image of a ChR2-expressing orexin cell before patching. (*B*) Robust spiking from a sample orexin cell (green) and no response from a control cell expressing mCherry alone (red) in response to 470-nm illumination. (Scale bar, 20 μM.)

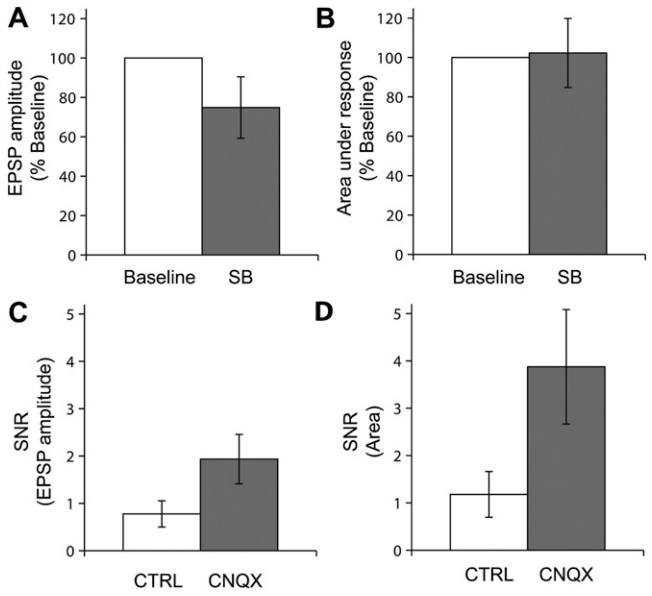

Fig. S4. (*A*) Bar plot indicating the effect of SB 334867 on initial EPSP amplitude ($n = 4$ cells from four animals). (*B*) Bar plot indicating the effect of SB 334867 on area under synaptic depolarization. (*C*) Signal-to-noise ratio (SNR) of the mean orexin contribution to EPSP amplitude (14%) relative to the SD of baseline responses in the presence (SD = 10 ± 4%, SNR = 1.94 ± 0.5) or absence (SD = 26 ± 7%, SNR = 0.78 ± 0.28) of 6-cyano-7-nitroquinoxaline-2,3-dione (CNQX). (*D*) SNR of the orexin contribution to the area under the response (21%) relative to the SD of the area in the presence (SD = 8 ± 3%, SNR = 3.88 ±1.2) or absence (SD = 28 ± 8%, SNR = 1.18 ± 0.48) of CNQX.